This journal is © the Owner Societies 2026

Supporting Information

Mechanistic Insights into High Performance W^{6+}-Doped Li_3YCl_6 Solid State Electrolyte: Synergy of Vacancy and Lattice Softening

Yile Ding,[‡a] Ziang Ren,[‡a] Shihui Zou,[a,d] Peng Shi,[b,d] Huadong Yuan,[a,d] Jianmin Luo,[a,d] Yujing Liu,[a,c] Jianwei Nai,[a,d] Xinyong Tao[a,d] and Yao Wang[*a,d]

a. College of Materials Science and Engineering, Zhejiang University of Technology, Hangzhou, 310014, China. wangyao@zjut.edu.cn

b. Science and Education Integration College of Energy and Carbon Neutrality, Zhejiang University of Technology, Hangzhou, 310014, China.

c. ZJUT-EXETER Joint Institute, Zhejiang University of Technology, Huzhou, 313000, China.

d. State Key Laboratory of Green Chemical Synthesis and Conversion.

‡ These authors contributed equally.

[*]Corresponding author: wangyao@zjut.edu.cn.

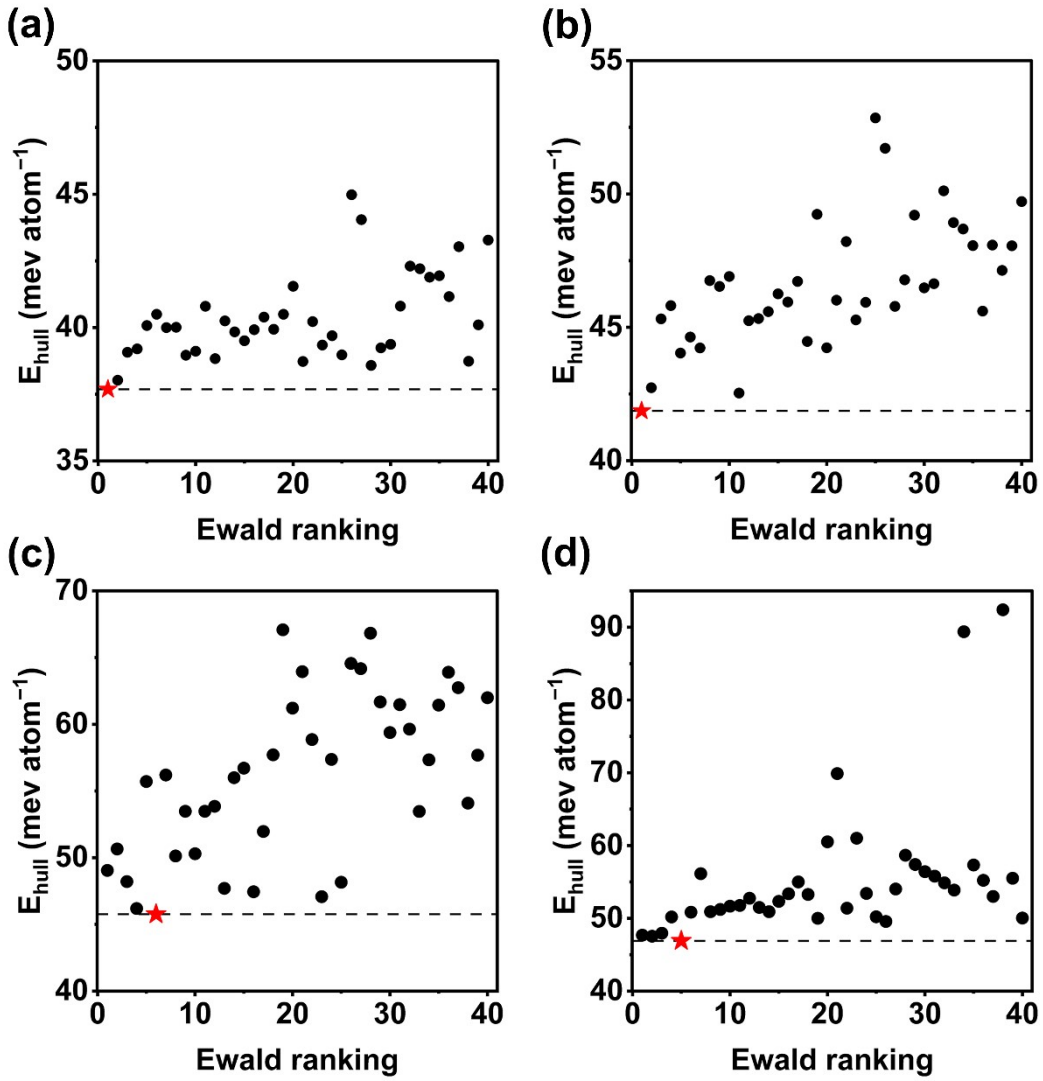

Fig. S1 E_{hull} as a function of Ewald ranking for (a) LYWC1 (b) LYWC2 (c) LYWC3 (d) LYWC4 systems. The dashed horizontal lines represent the energy reference, and red stars indicate the most stable structures selected for further calculations.

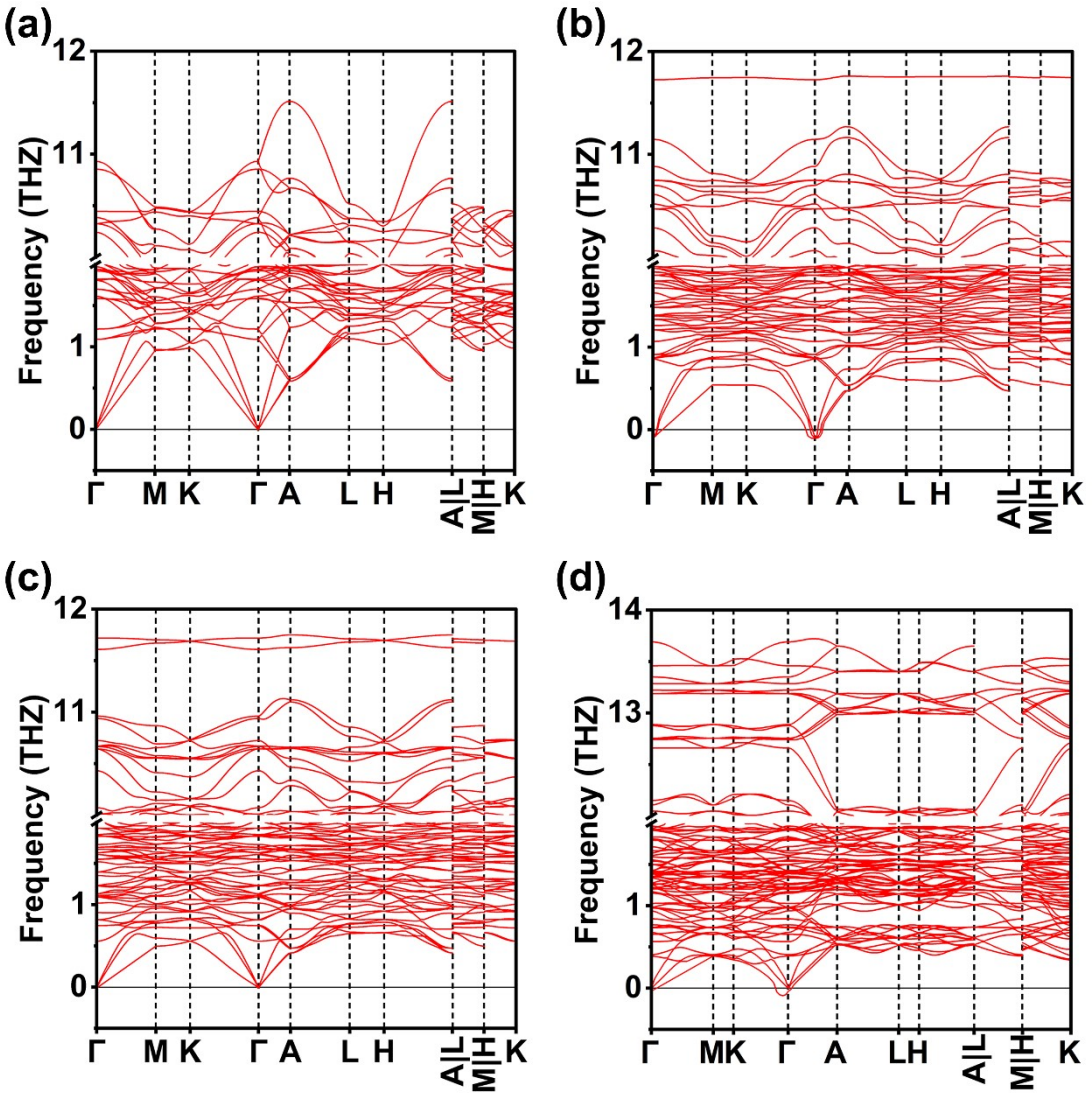

Fig. S2 The phonon dispersion spectra of (a) LYC, (b) LYWC1, (c) LYWC3, and (d) LYWC4.

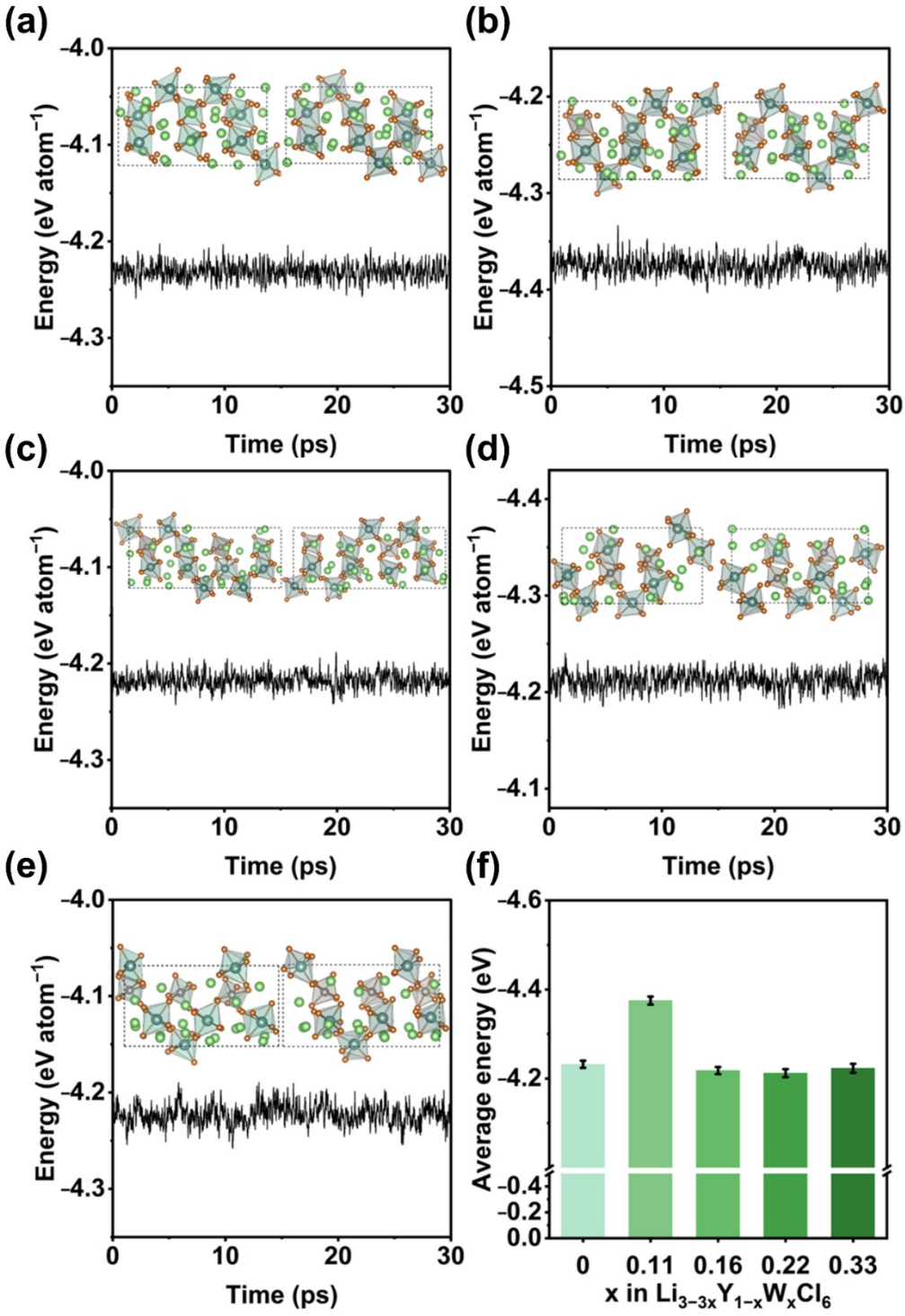

Fig. S3 Energy fluctuations (700 K AIMD) for (a) LYC, (b) LYWC1, (c) LYWC2, (d) LYWC3 and (e) LYWC4 (f) Standard deviations and error bars of the energy fluctuation.

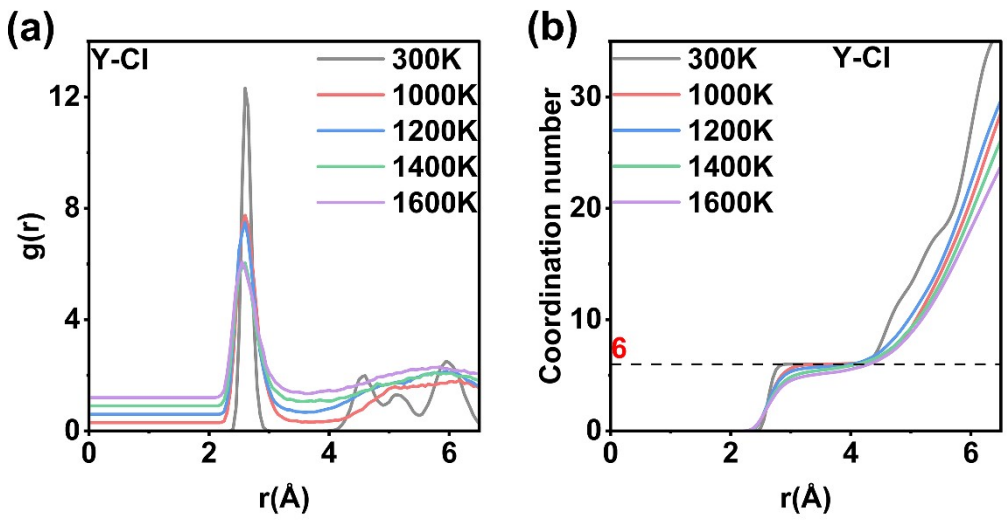

Fig. S4 (a) The radial distribution function of Y-Cl in LYC. (b) The integral of the radial distribution function of Y-Cl in LYC.

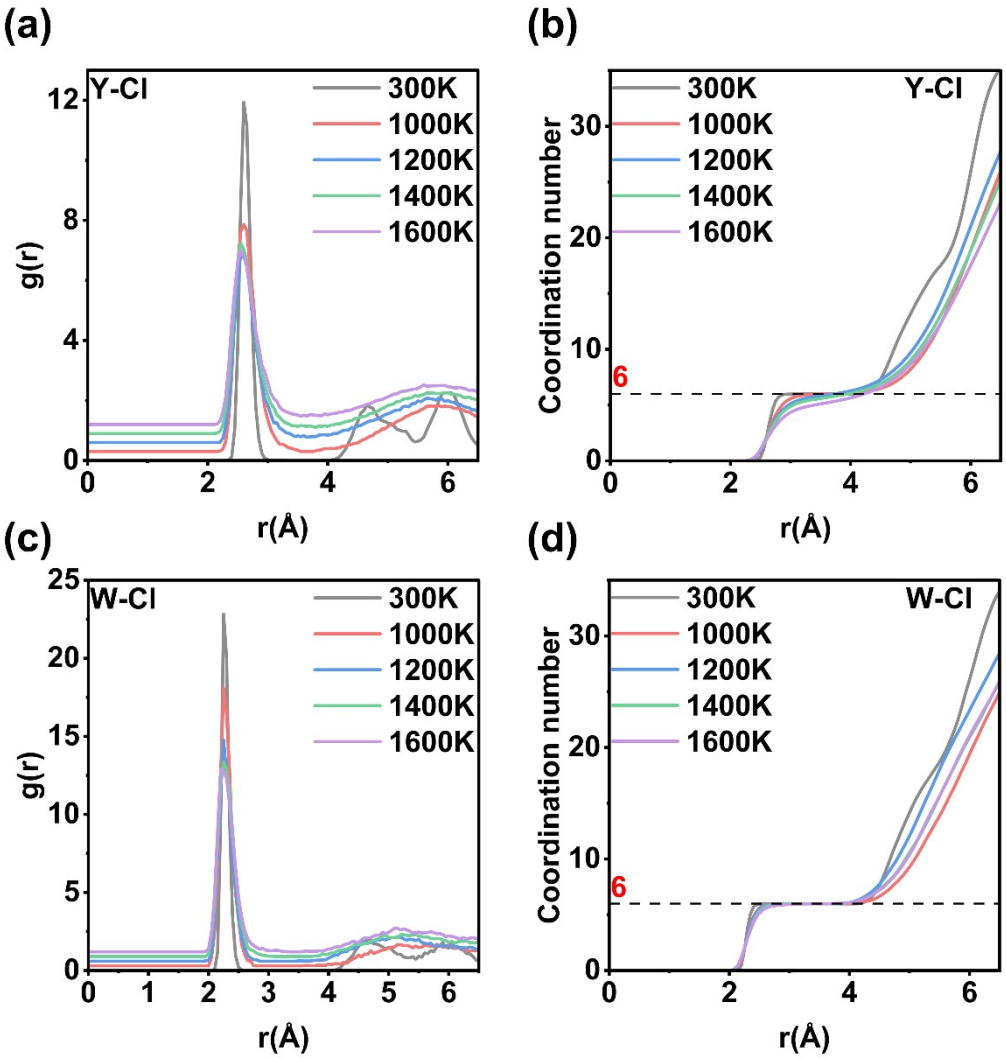

Fig. S5 (a, b) The radial distribution function and the integral of the radial distribution function of Y-Cl, (c, d) The radial distribution function and the integral of the radial distribution function of W-Cl in LYWC1.

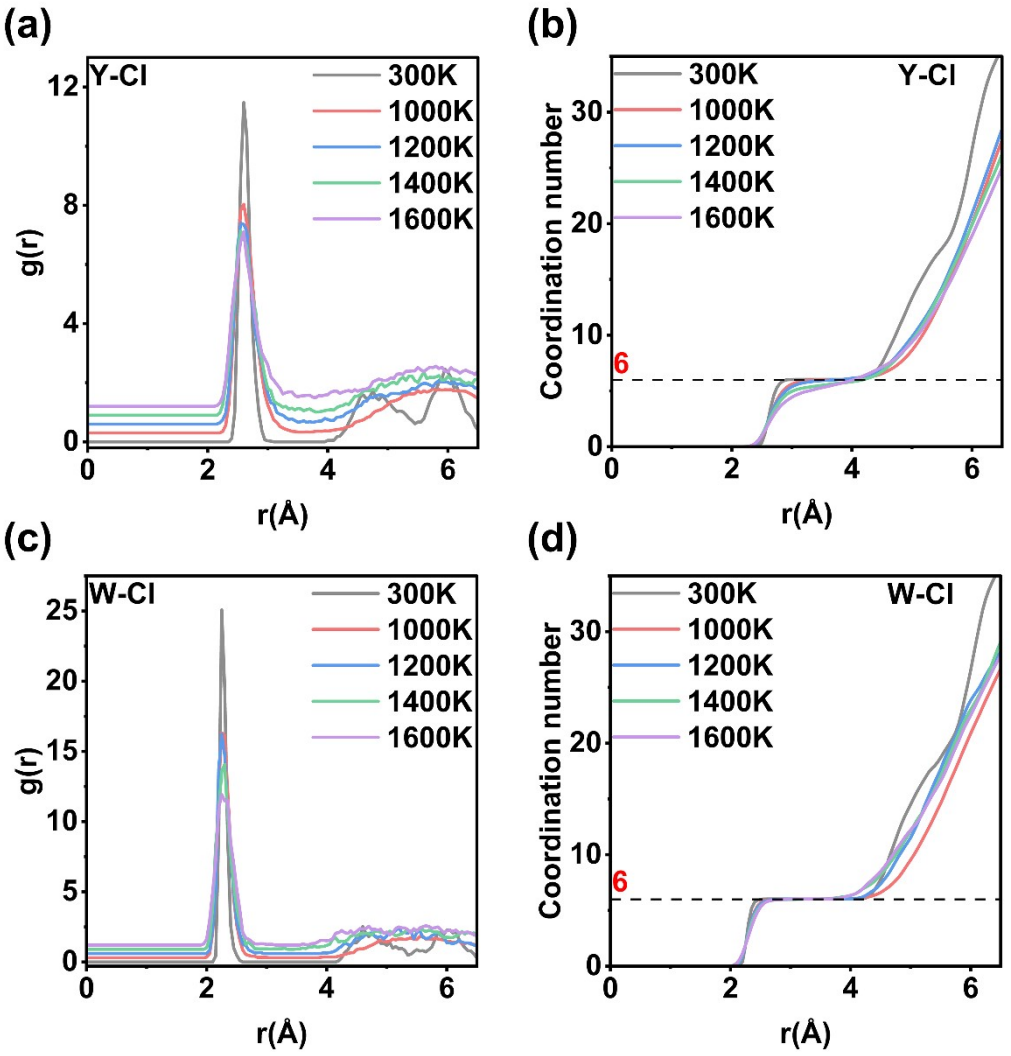

Fig. S6 (a, b) The radial distribution function and the integral of the radial distribution function of Y-Cl, (c, d) The radial distribution function and the integral of the radial distribution function of W-Cl in LYWC2.

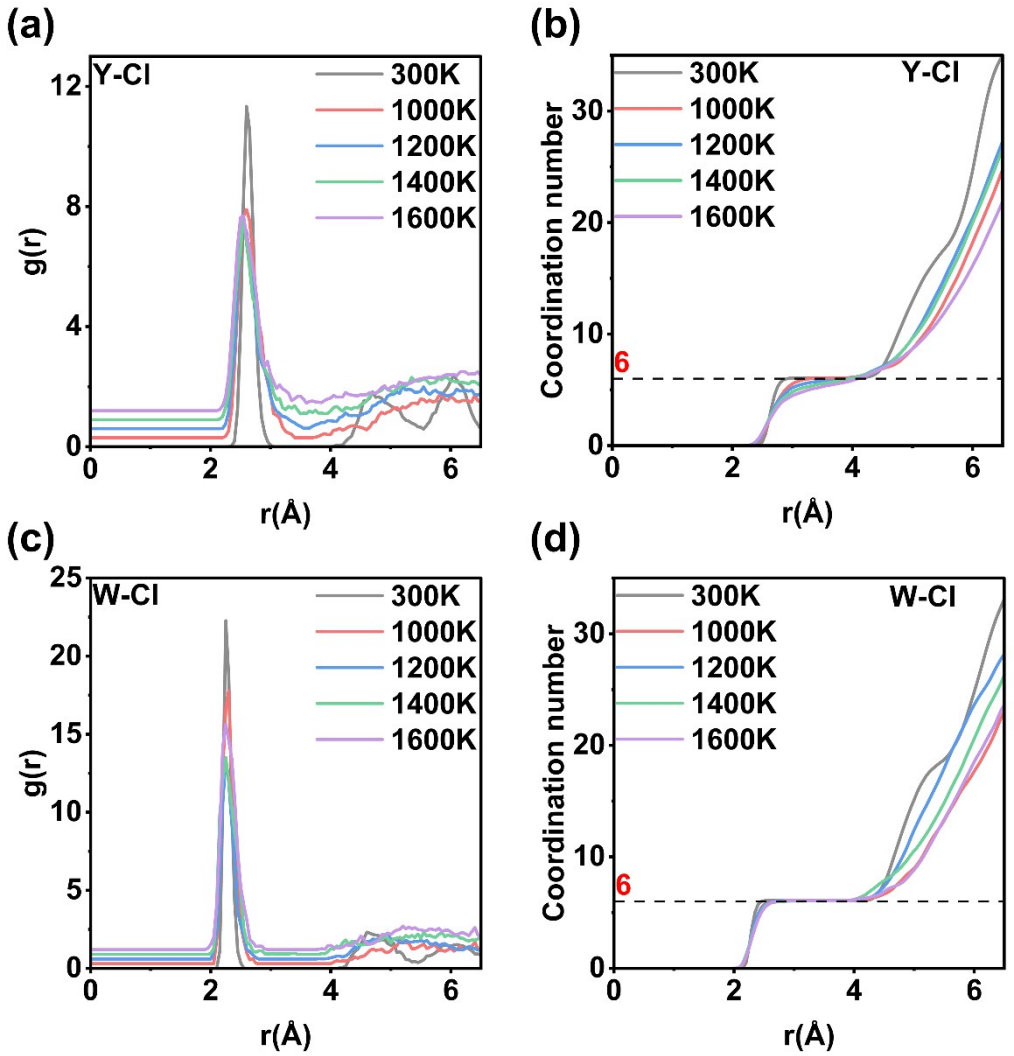

Fig. S7 (a, b) The radial distribution function and the integral of the radial distribution function of Y-Cl, (c, d) The radial distribution function and the integral of the radial distribution function of W-Cl in LYWC3.

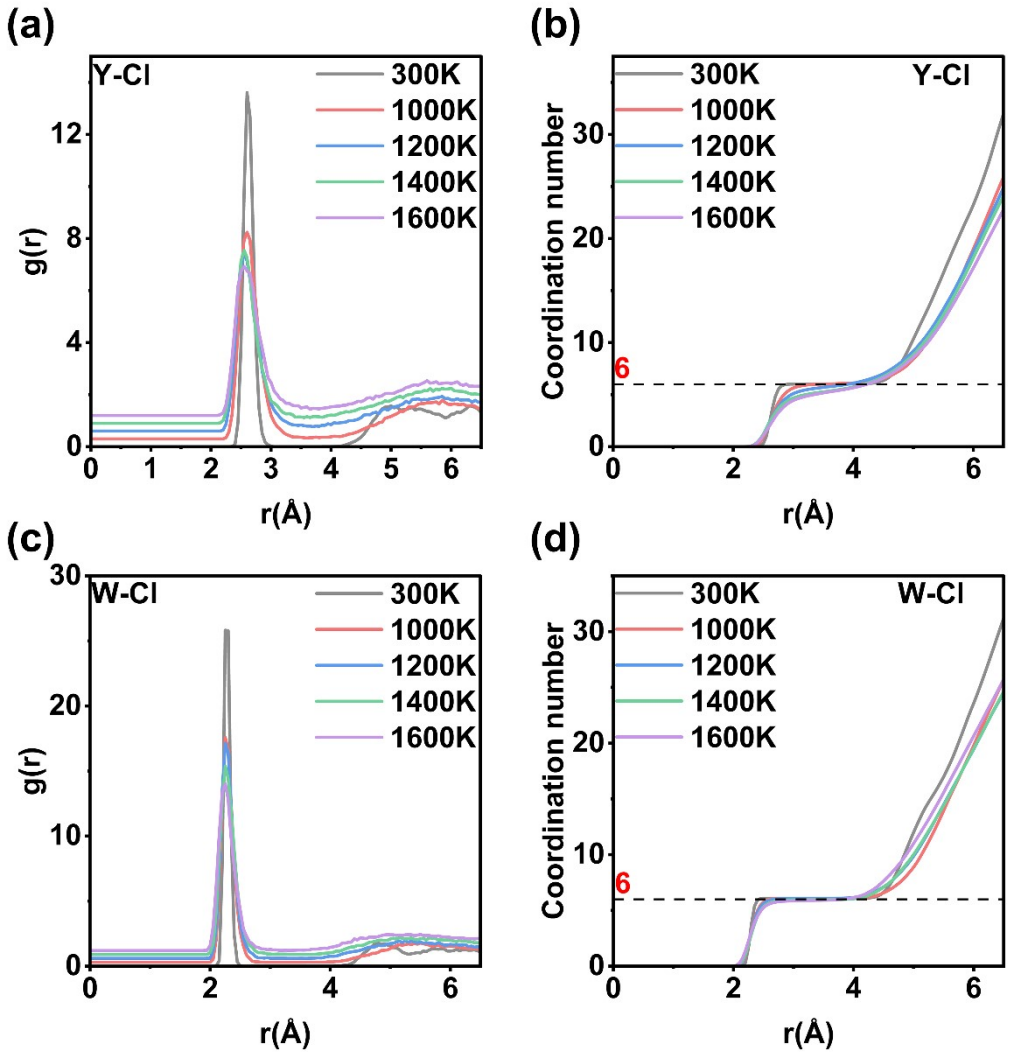

Fig. S8 (a, b) The radial distribution function and the integral of the radial distribution function of Y-Cl, (c, d) The radial distribution function and the integral of the radial distribution function of W-Cl in LYWC4.

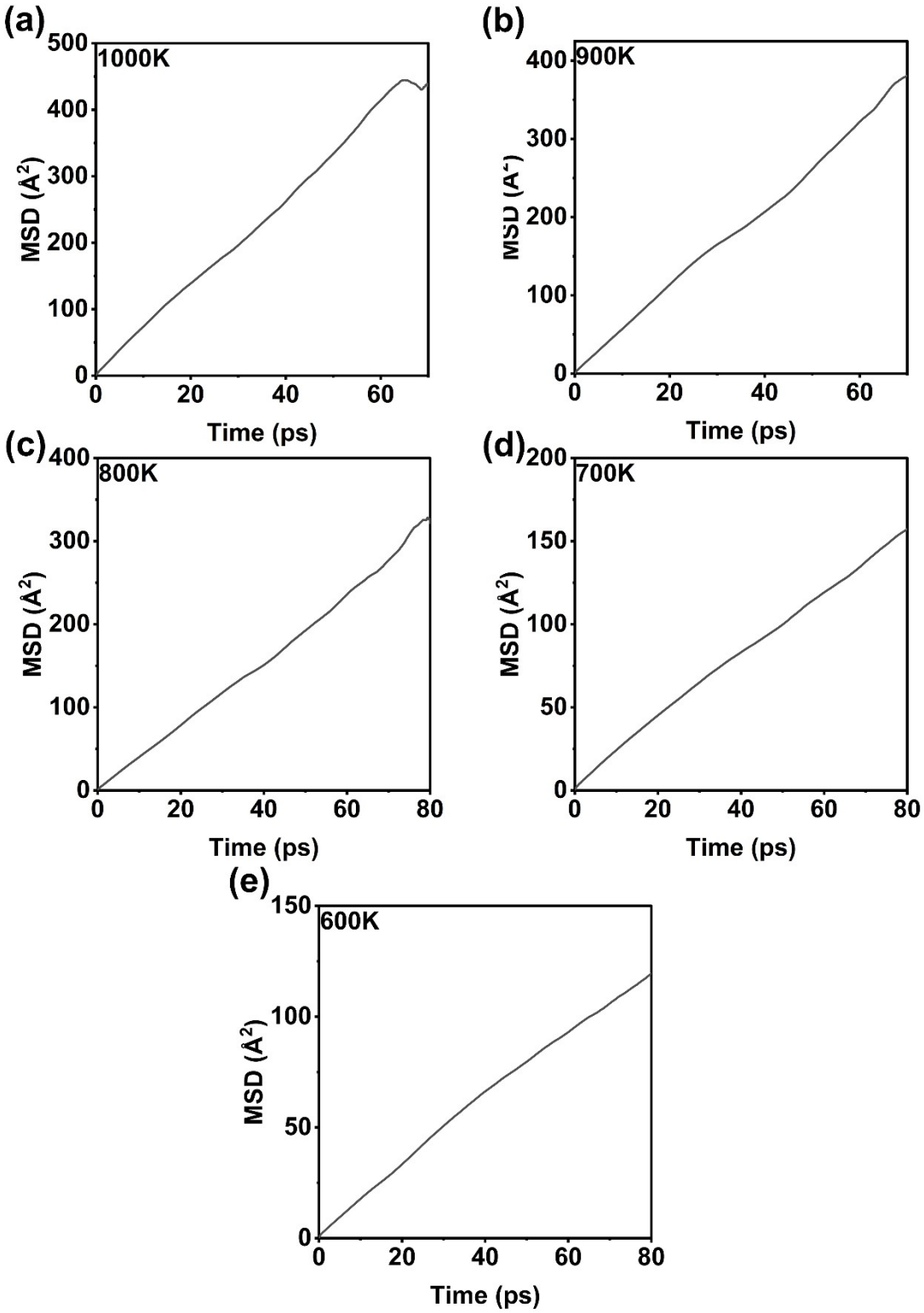

Fig. S9 Li^+ MSD plots of LYC for AIMD simulations. (a) 70ps AIMD simulation at 1000K. (b) 70ps AIMD simulation at 900K. (c) 80ps AIMD simulation at 800K. (d) 80ps AIMD simulation at 700K. (e) 80ps AIMD simulation at 600K.

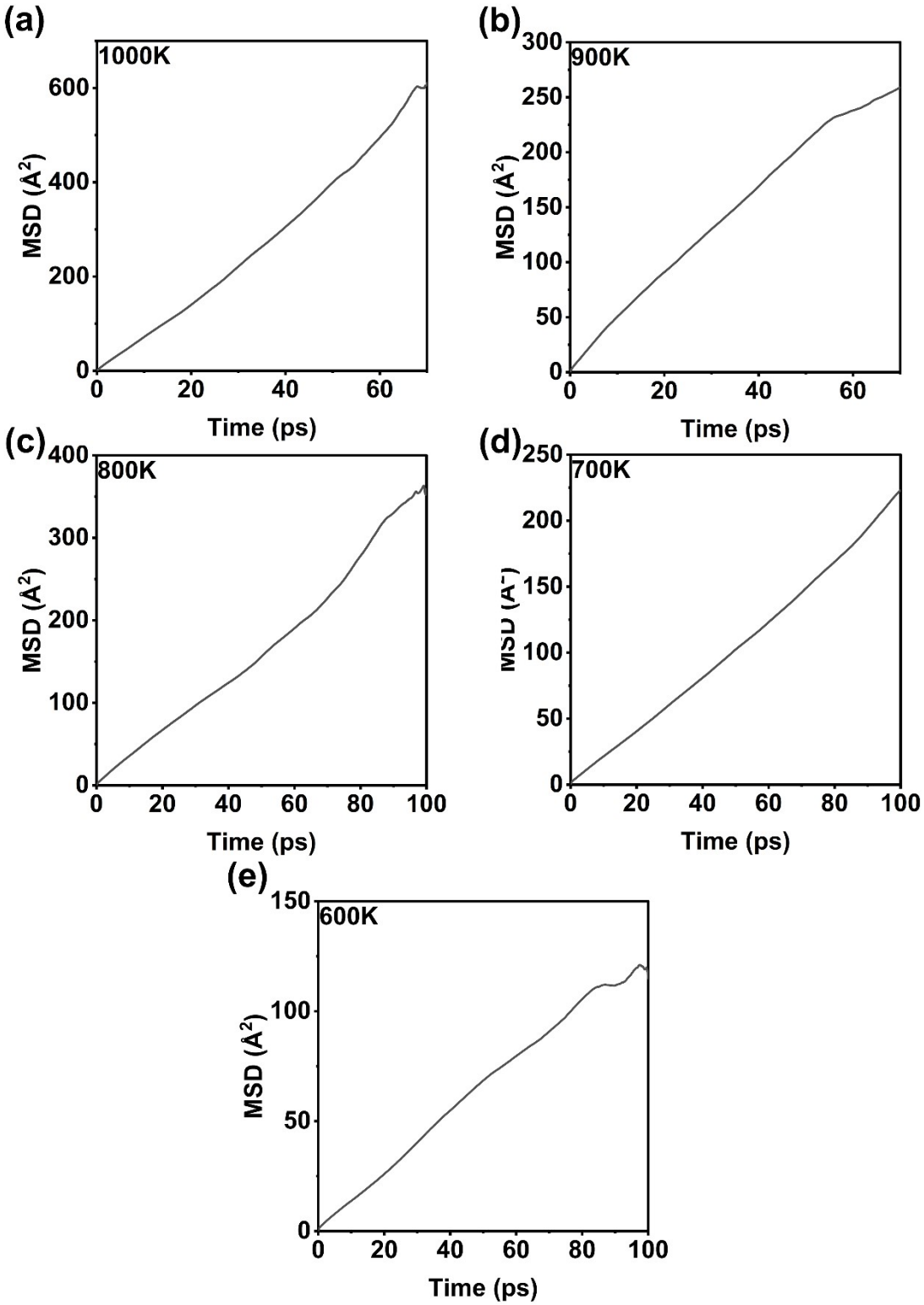

Fig. S10 Li^+ MSD plots of LYWC1 for AIMD simulations. (a) 70ps AIMD simulation at 1000K. (b) 70ps AIMD simulation at 900K. (c) 100ps AIMD simulation at 800K. (d) 100ps AIMD simulation at 700K. (e) 100ps AIMD simulation at 600K.

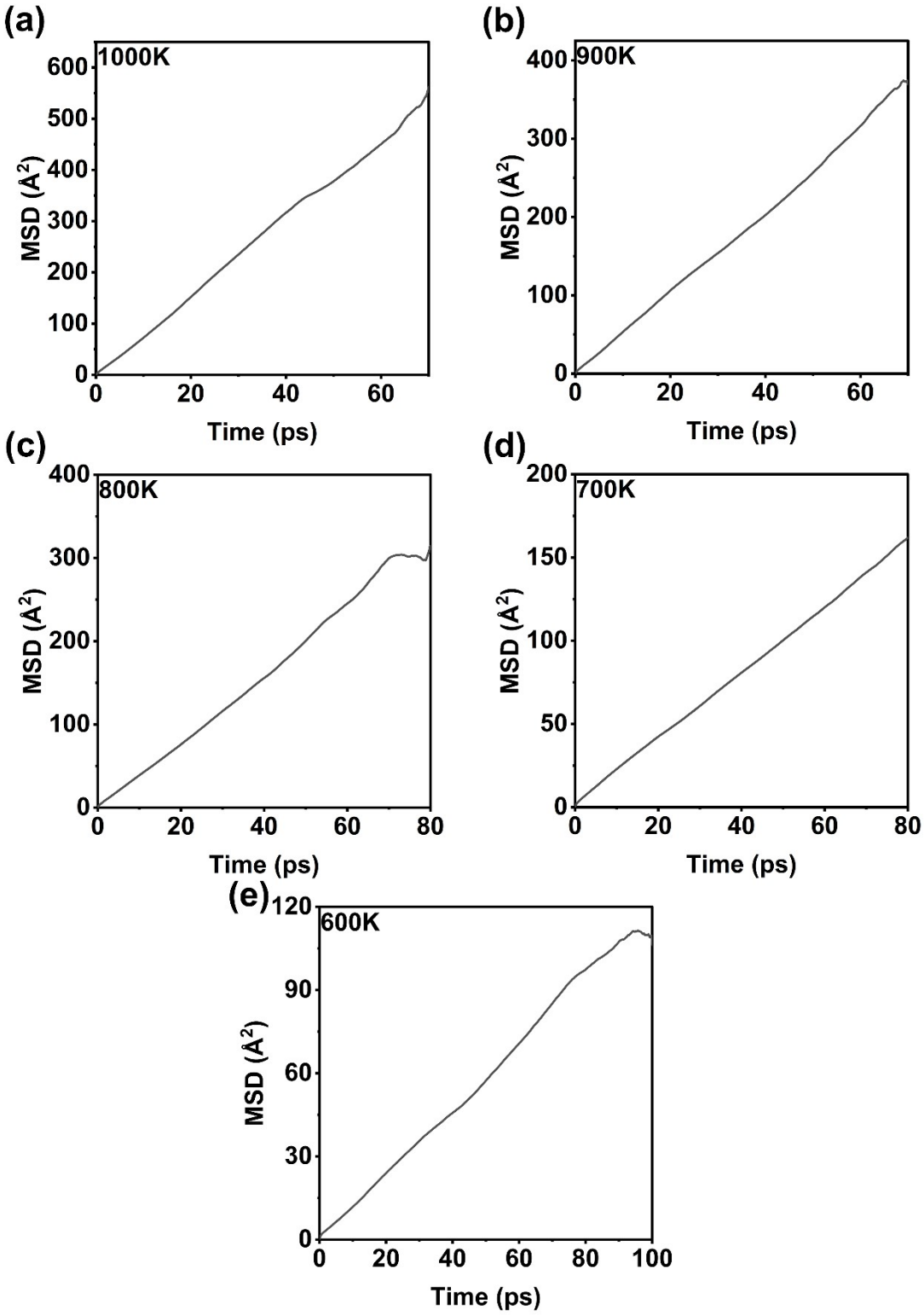

Fig. S11 Li^+ MSD plots of LYWC2 for AIMD simulations. (a) 70ps AIMD simulation at 1000K. (b) 70ps AIMD simulation at 900K. (c) 80ps AIMD simulation at 800K. (d) 80ps AIMD simulation at 700K. (e) 100ps AIMD simulation at 600K.

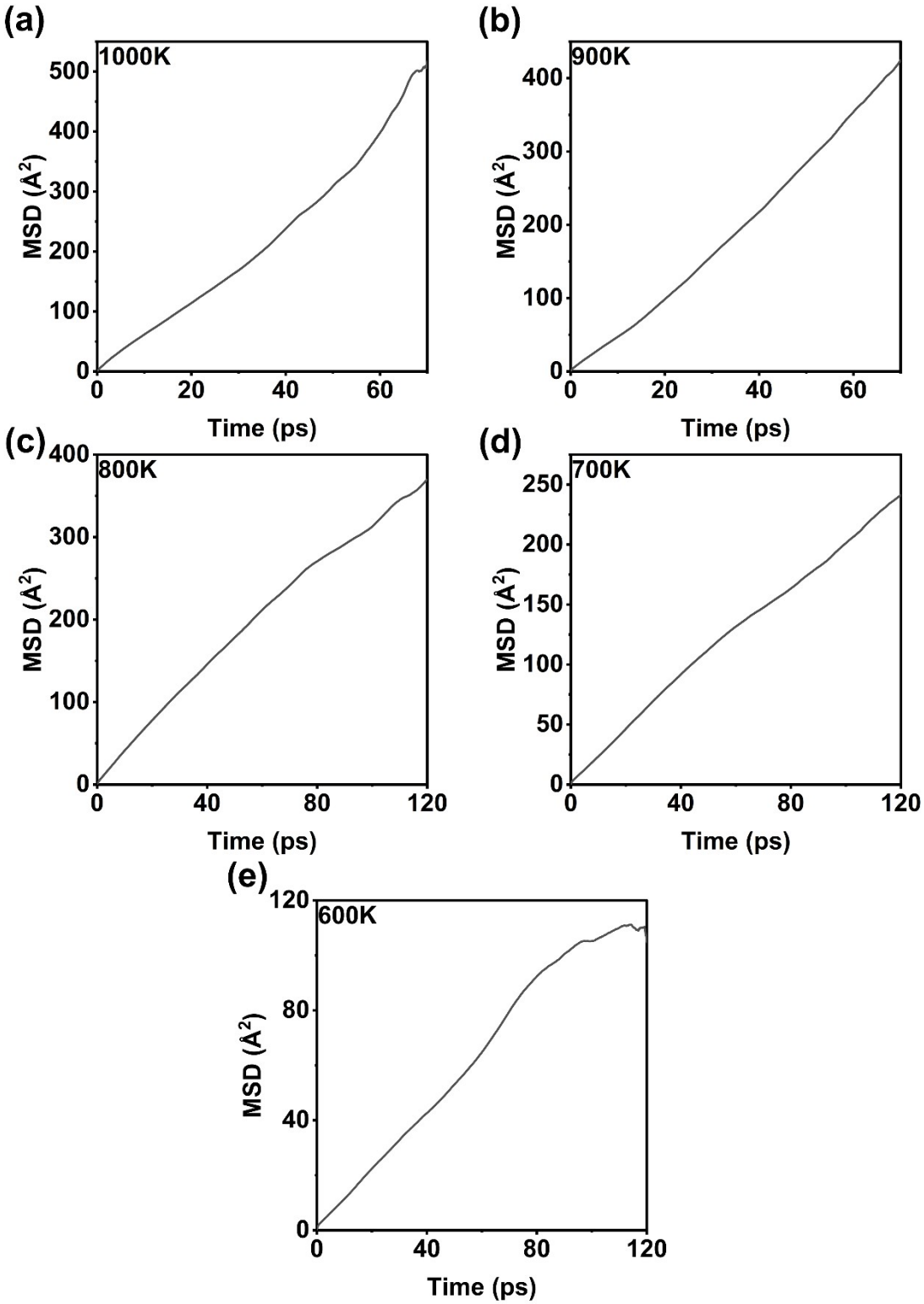

Fig. S12 Li^+ MSD plots of LYWC3 for AIMD simulations. (a) 70ps AIMD simulation at 1000K. (b) 70ps AIMD simulation at 900K. (c) 120ps AIMD simulation at 800K. (d) 120ps AIMD simulation at 700K. (e) 120ps AIMD simulation at 600K.

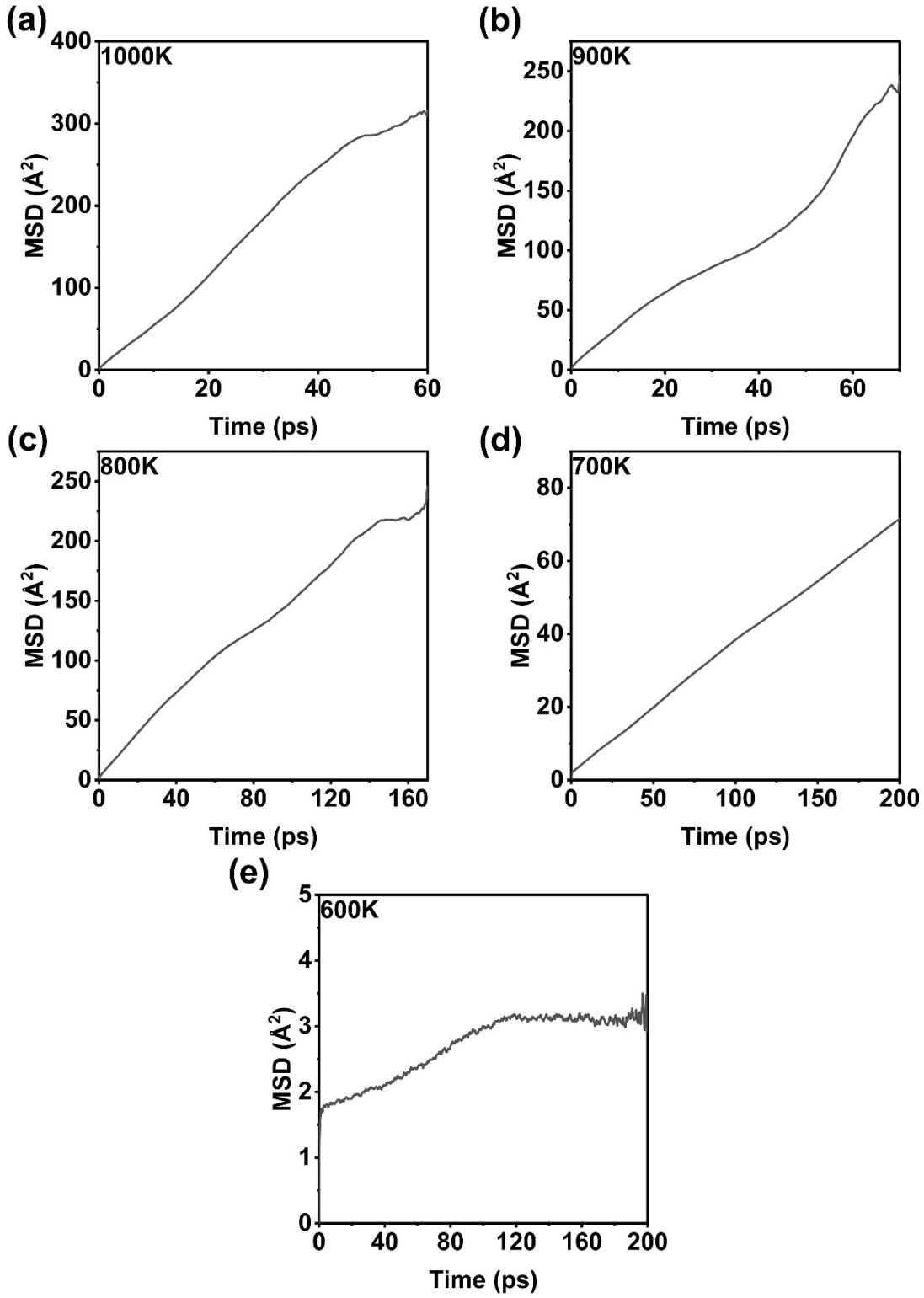

Fig. S13 Li^+ MSD plots of LYWC4 for AIMD simulations. (a) 70ps AIMD simulation at 1000K. (b) 70ps AIMD simulation at 900K. (c) 170ps AIMD simulation at 800K. (d) 200ps AIMD simulation at 700K. (e) 200ps AIMD simulation at 600K.

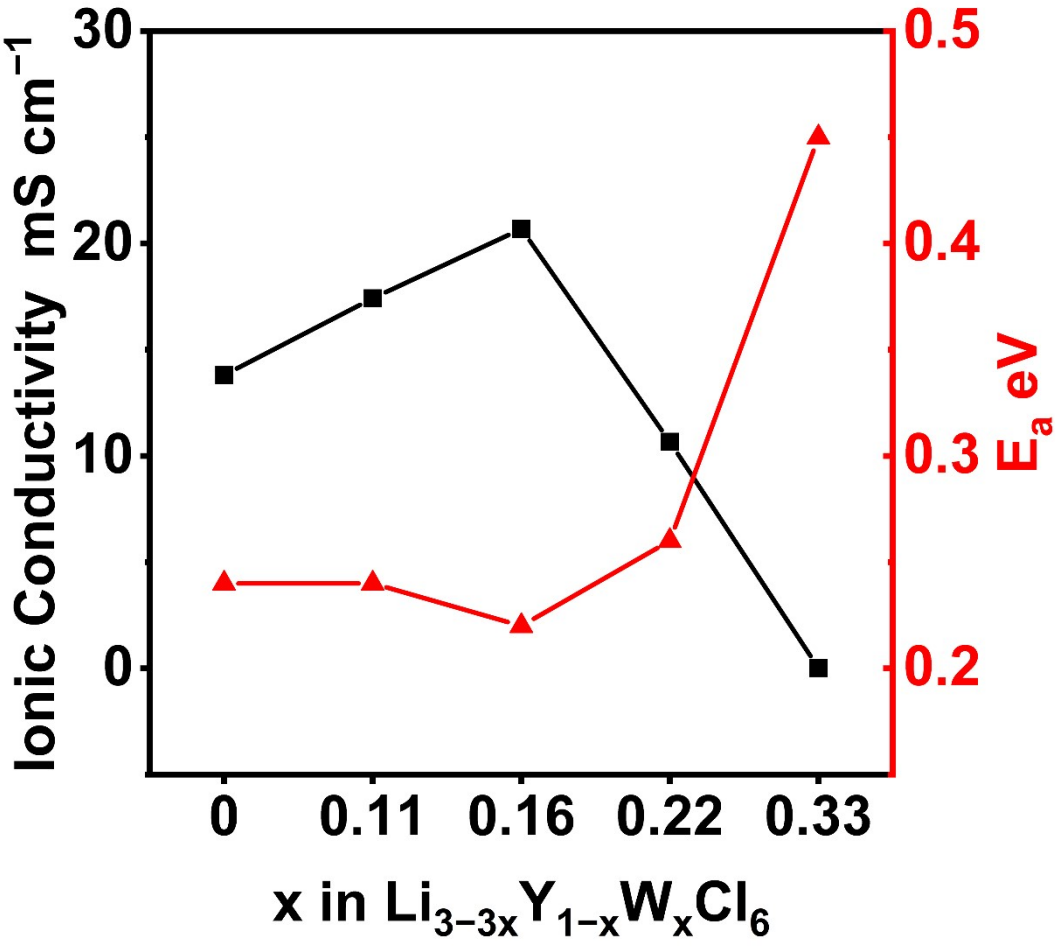

Fig. S14 Li^+ conductivities and activation energies for different doping structures from AIMD simulations in values at 300 K.

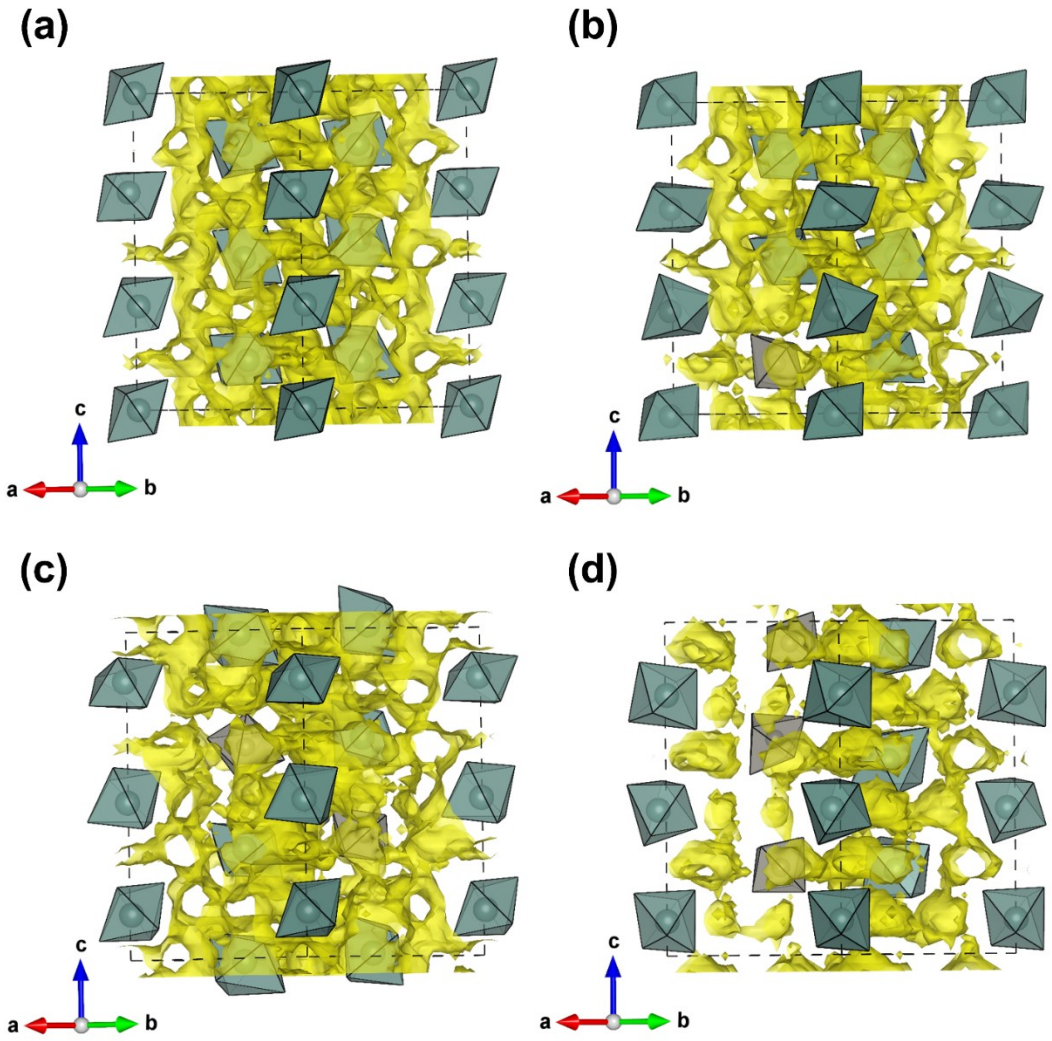

Fig. S15 The Li^+ probability density at 700K obtained by AIMD simulation (yellow) is superimposed on the anion sublattices of (a) LYC, (b) LYWC1, (c) LYWC3, and (d) LYWC4.

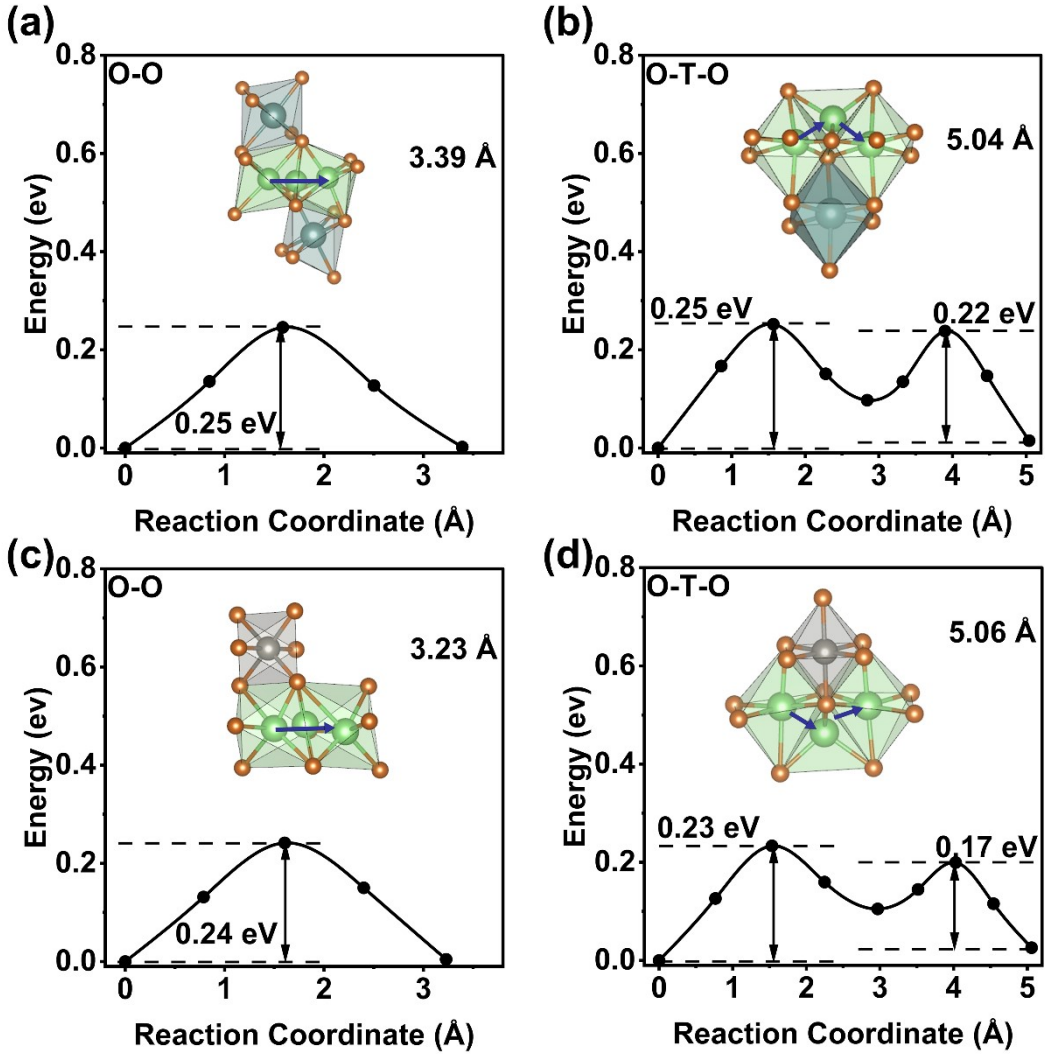

Fig. S16 Migration energy barrier diagrams with Cl-NEB calculations, (a, b) O-O and O-T-O pathways around Y atoms, (c, d) O-O and O-T-O pathways around W atoms in LYWC1.

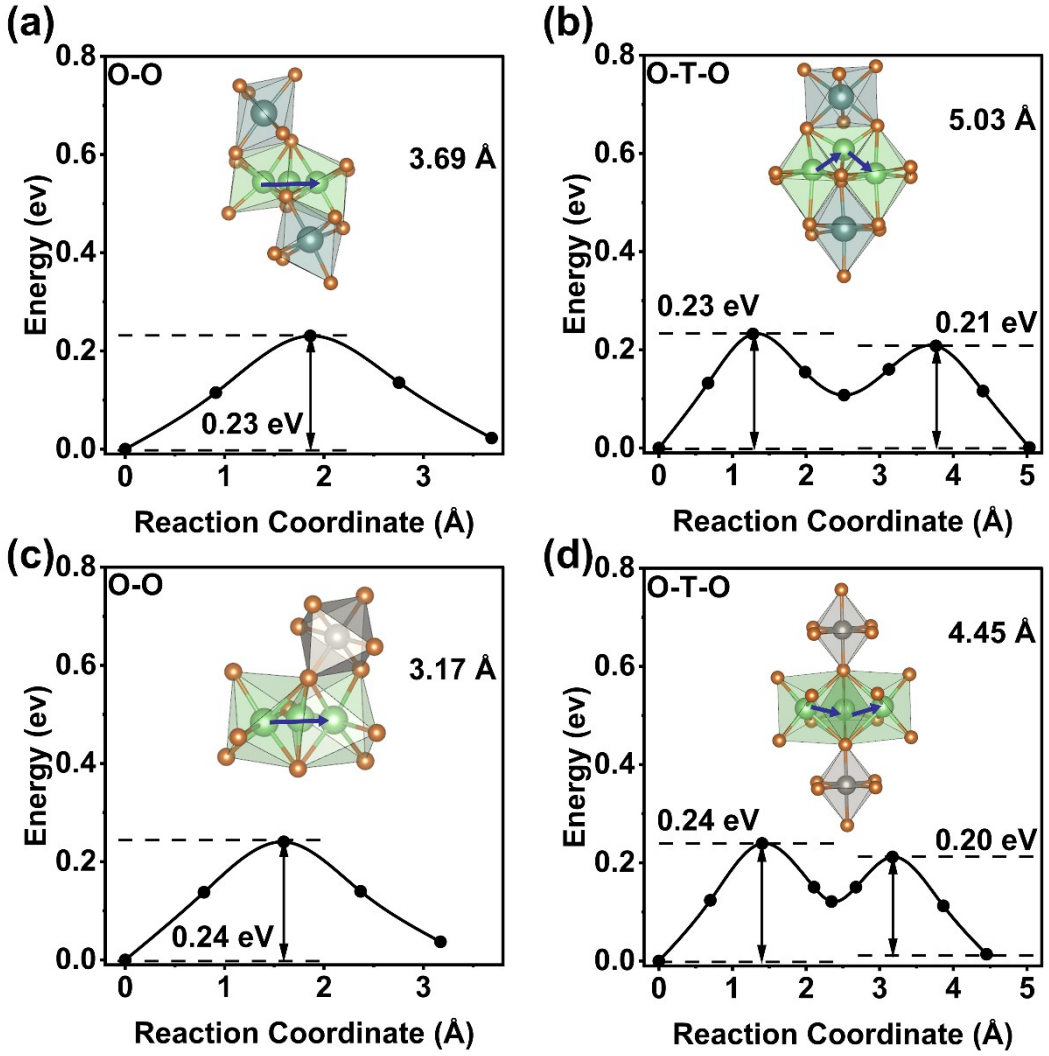

Fig. S17 Migration energy barrier diagrams with Cl-NEB calculations, (a, b) O-O and O-T-O pathways around Y atoms, (c, d) O-O and O-T-O pathways around W atoms in LYWC3.

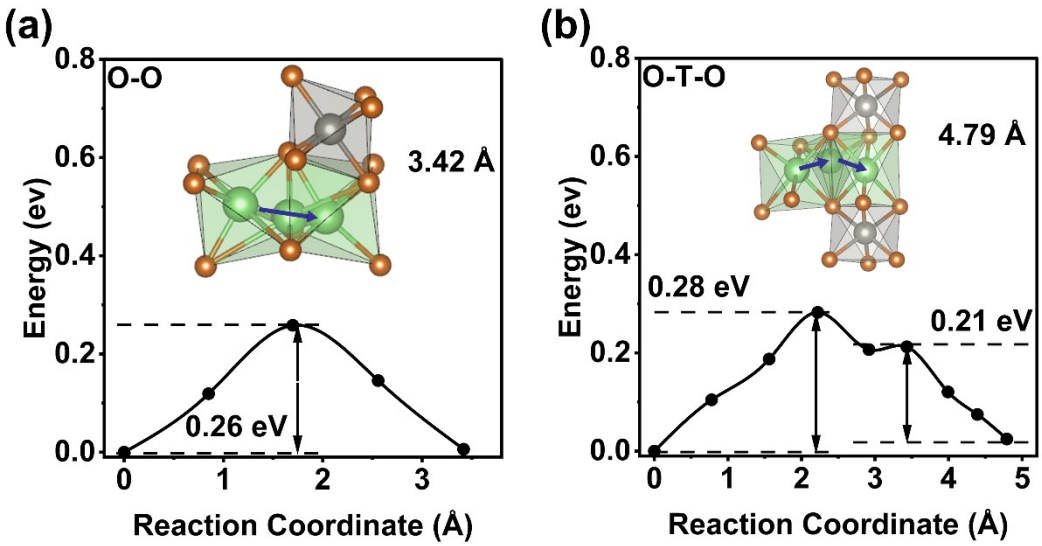

Fig. S18 Migration energy barrier diagrams with Cl-NEB calculations, (a, b) O-O and O-T-O pathways around Y atoms, (c, d) O-O and O-T-O pathways around W atoms in LYWC4.

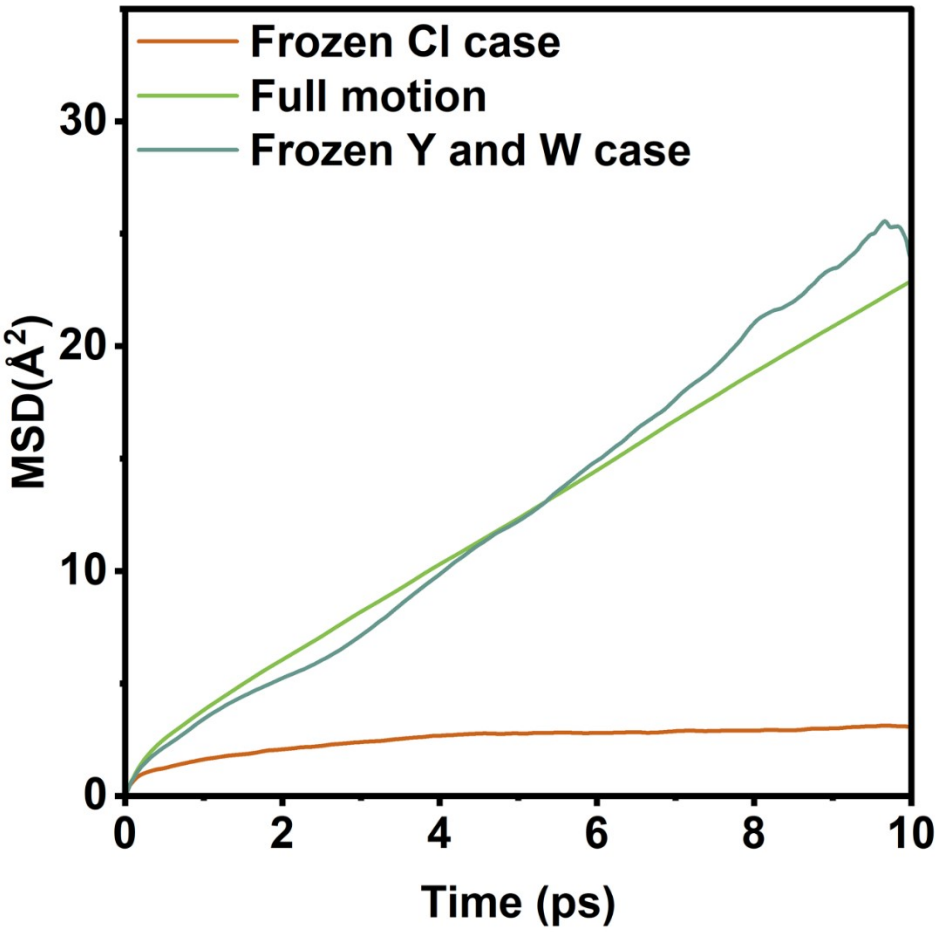

Fig. S19 mean square displacement (MSD) of Li^+ in the LYWC2 structure under both full motion and frozen chloride ion framework conditions.

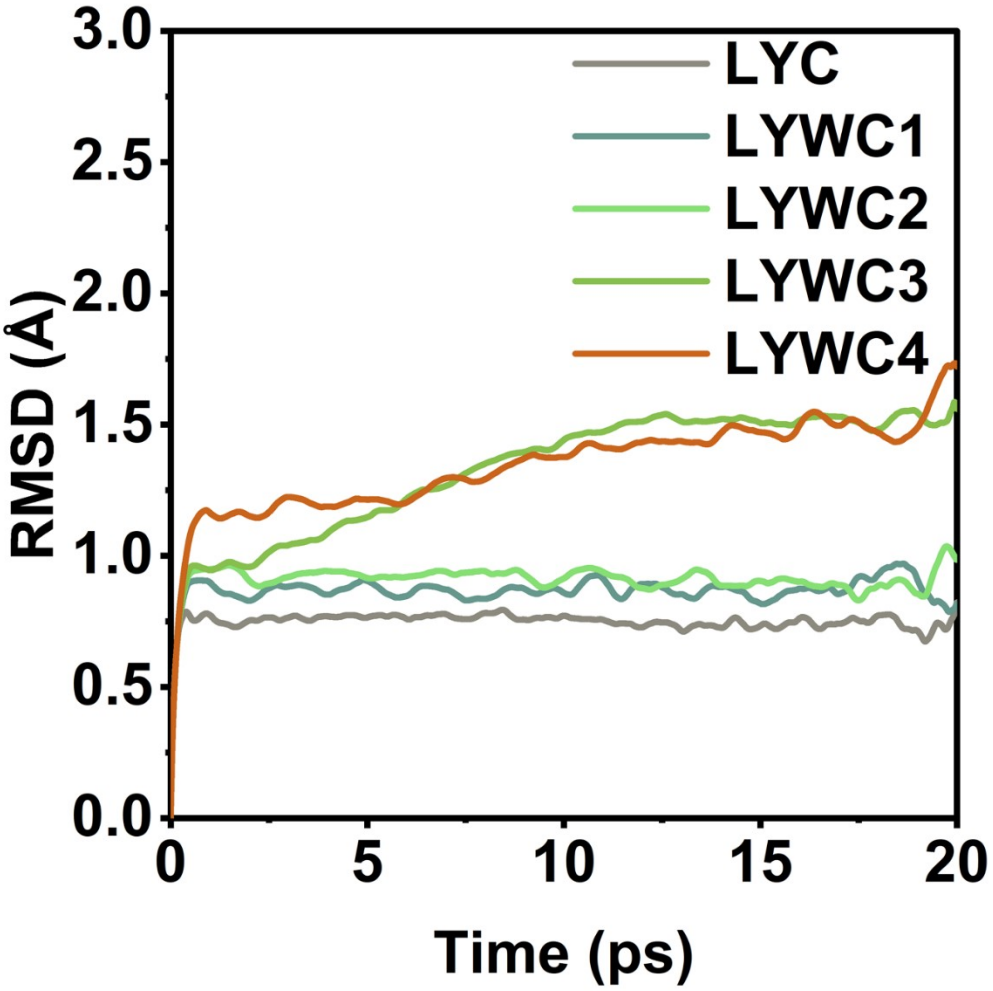

Fig. S20 RMSD of Cl^- in LYWC at 700 K

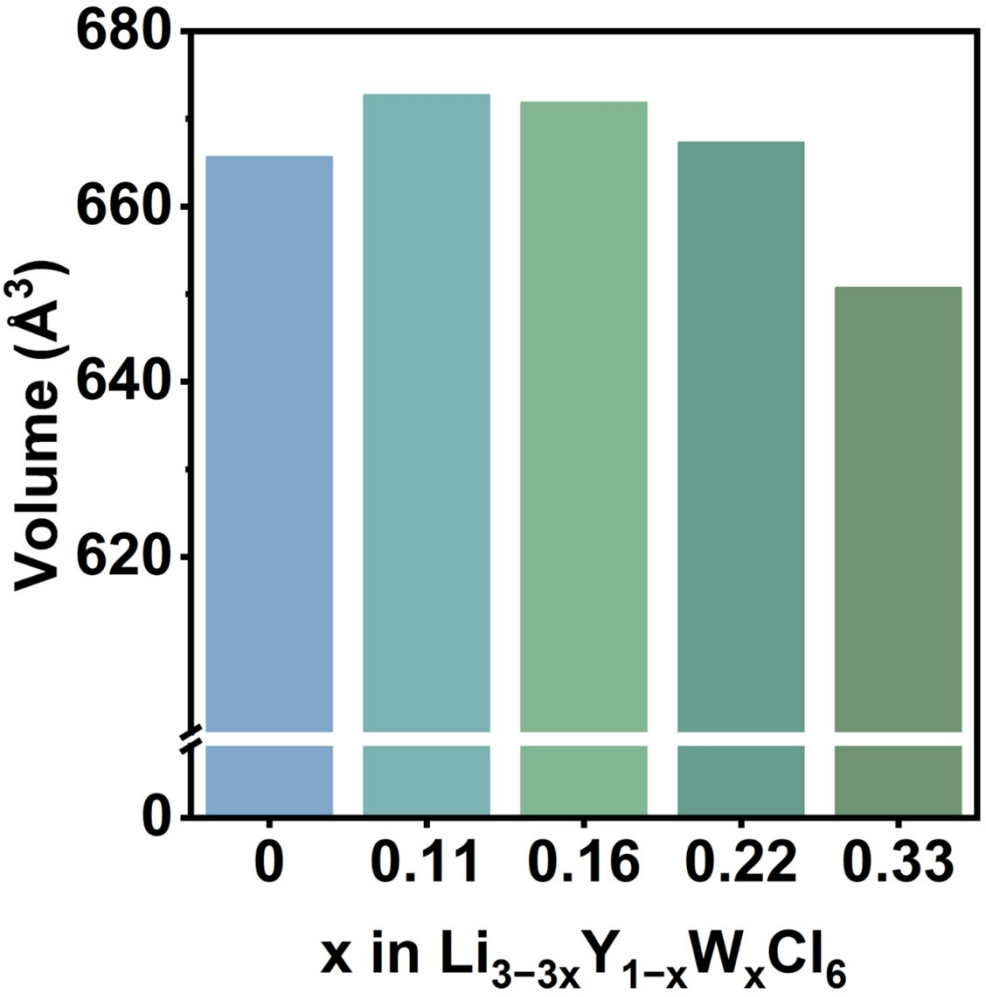

Fig. S21 Variation of unit cell volume with doping concentration in the LYWC structure.

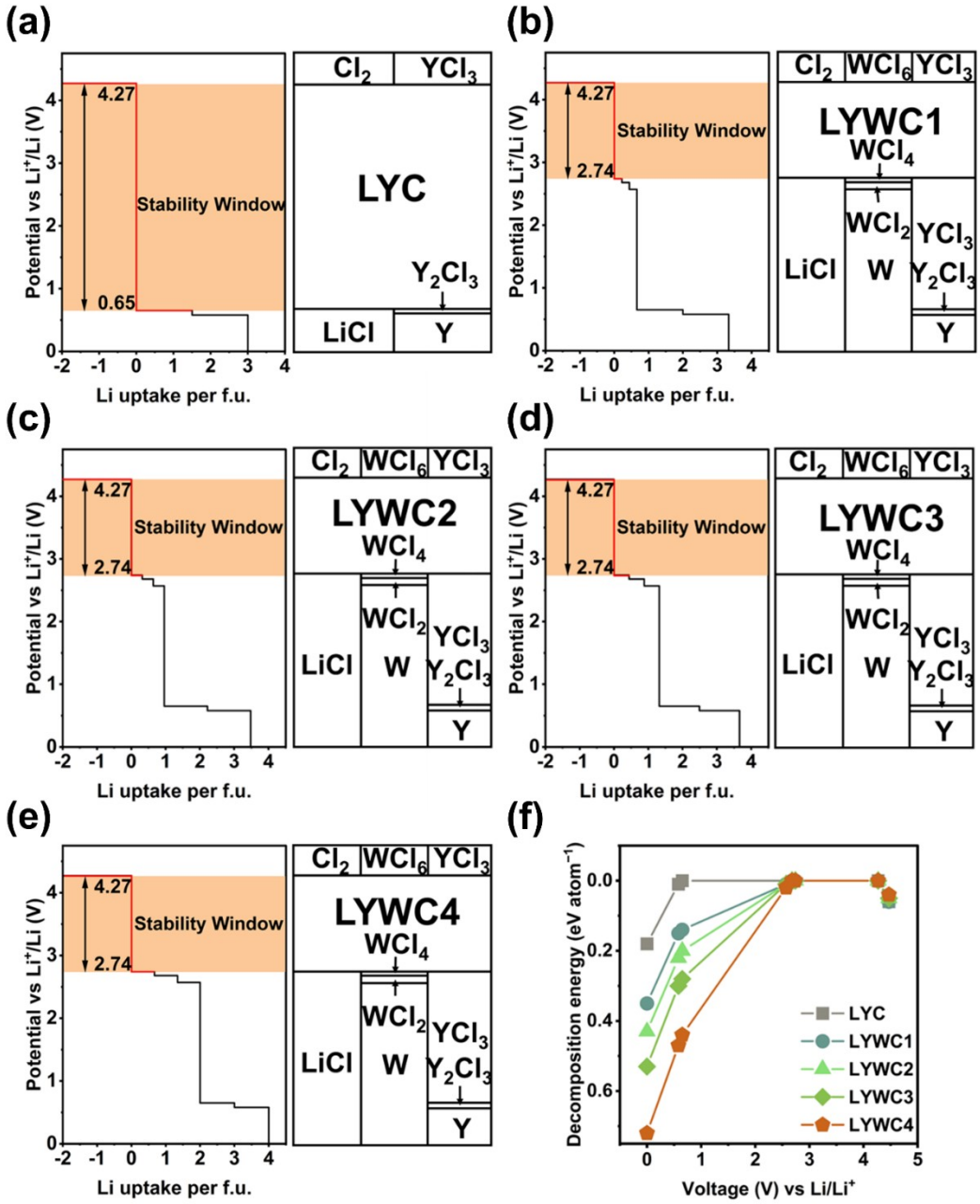

Fig. S22 The thermodynamic profiles and phase equilibria for (a) LYC (b) LYWC1, (c) LYWC2, (d) LYWC3 and (e) LYWC4. (f) The decomposition energy of LYWC as a function of the chemical potential of Li^+.

Table S1 Values of global maximum pore cavity diameter (GCD), largest cavity diameter (LCD), and pore-limiting diameter (PLD) for LYWC.

System	GCD (Å)	LCD (Å)	PLD (Å)
LYC	1.14	1.04	0.54
LYWC1	1.25	1.25	0.57
LYWC2	1.25	1.14	0.58
LYWC3	1.20	1.13	0.61
LYWC4	1.11	0.80	0.65

Table S2 Percolation radius, ionic conductivity of different systems

System	P_r (Å)	σ at 300 K (mS cm^{-1})
Li_3SmCl_6	0.64	15.45[1]
Li_2HfCl_6	0.51	0.50[2]
Li_2ZrCl_6	0.51	1.00[2]
Li_3InCl_6	0.54	6.40[3]
Li_3ScCl_6	0.56	29.00[4]
$LiSbCl_6$	0.71	69.70[5]
Li_3YCl_6	0.54	13.81
LYWC1	0.57	17.42
LYWC2	0.58	20.69
LYWC3	0.61	10.67
LYWC4	0.65	0.02

Table S3 Inradius of [$LiCl_6$] with different doping structures

Composition	Diffusion paths (Å)			
	O-O		O-T-O	
	Around the Y	Around the W	Around the Y	Around the W
LYC	2.18	/	0.78	/
LYWC1	2.21	2.17	0.79	0.82
LYWC2	2.23	2.23	0.81	0.82
LYWC3	2.22	2.22	0.79	0.78
LYWC4	/	2.16	/	0.74

Table S4 Ionic conductivity, phonon band center, and bulk modulus of different systems

System	phonon band center (THz)	bulk modulus (GPa)	σ at 300 K (mS cm^{-1})
Li_3InCl_6	/	16.13[6]	6.40[3]
Li_3ScCl_6	/	17.85[6]	29.00[4]
Li_3YCl_6	5.11	21.20	13.81
LYWC1	5.04	17.49	17.42
LYWC2	4.96	15.66	20.69
LYWC3	5.00	15.53	10.67
LYWC4	5.82	18.34	0.02
Li_3ErBr_6	/	11.53[6]	1.00[7]
$LiNbOCl_4$	/	22.70[8]	17.40[8]
Li_6PS_5Cl	/	28.00[9]	2.59[10]
$Li_{10}Ge(PS_6)_2$	/	25.00[9]	12.00[11]

Table S5 Chemical reactions, decomposition phases, and decomposition energy (E_D), between LYWC, sulfides (Li_3PS_4, $Li_{10}Ge(PS_6)_2$, and Li_6PS_5Cl), and cathode materials ($LiFePO_4$ (LFP),

Cathode	SSE	Reaction equation	E_D (meV atom^{-1})
LFP	LYC	$0.3333\ Li_3YCl_6 + 0.6667\ LiFePO_4 \rightarrow 0.3333\ Fe_2PClO_4 + 0.3333\ YPO_4 + 1.667\ LiCl$	−29.00
	LYWC1	$0.6403\ LiFePO_4 + 0.3597\ Li_{2.67}Y_{0.89}W_{0.11}Cl_6 \rightarrow 0.03957\ WCl_6 + 0.3201\ YPO_4 + 0.3201\ Fe_2PClO_4 + 1.601\ LiCl$	−28.00
	LYWC2	$0.6269\ LiFePO_4 + 0.3731\ Li_{2.52}Y_{0.84}W_{0.16}Cl_6 \rightarrow 0.0597\ WCl_6 + 0.3134\ YPO_4 + 0.3134\ Fe_2PClO_4 + 1.567\ LiCl$	−27.00
	LYWC3	$0.6094\ LiFePO_4 + 0.3906\ Li_{2.34}Y_{0.78}W_{0.22}Cl_6 \rightarrow 0.08594\ WCl_6 + 0.3047\ YPO_4 + 0.3047\ Fe_2PClO_4 + 1.523\ LiCl$	−27.00
	LYWC4	$0.5726\ LiFePO_4 + 0.4274\ Li_{2.01}Y_{0.67}W_{0.33}Cl_6 \rightarrow 0.141\ WCl_6 + 0.2863\ YPO_4 + 0.2863\ Fe_2PClO_4 + 1.432\ LiCl$	−25.00
	Li_3PS_4	$0.3\ Li_3PS_4 + 0.7\ LiFePO_4 \rightarrow 0.4\ Li_4P_2O_7 + 0.2\ FePS + 0.5\ FeS_2$	−85.00
	$Li_{10}Ge(PS_6)_2$	$0.1463\ Li_{10}Ge(PS_6)_2 + 0.8537\ LiFePO_4 \rightarrow 0.1951\ Li_4P_2O_7 + 0.5122\ Li_3PO_4 + 0.2439\ FePS + 0.1463\ GeS_2 + 0.6098\ FeS_2$	−101.00
	Li_6PS_5Cl	$0.2857\ Li_6PS_5Cl + 0.7143\ LiFePO_4 \rightarrow 0.1818\ FePS + 0.02597\ P_4S_7 + 0.7143\ Li_3PO_4 + 0.5325\ FeS_2 + 0.2857\ LiCl$	−136.00

Table S6 Chemical reactions, decomposition phases, and decomposition energy (E_D), between LYWC, sulfides (Li_3PS_4, $Li_{10}Ge(PS_6)_2$, and Li_6PS_5Cl), and four cathode materials $LiMn_2O_4$ (LMO).

Cathode	SSE	Reaction equation	E_D (meV atom^{-1})
LMO	LYC	0.2857 Li_3YCl_6 + 0.7143 $LiMn_2O_4$ → 0.2857 YMn_2O_5 + 0.04762 $Mn_8Cl_3O_{10}$ + 0.4762 MnO_2 + 1.571 LiCl	−15.00
	LYWC1	0.7312 $LiMn_2O_4$ + 0.2688 $Li_{2.67}Y_{0.89}W_{0.11}Cl_6$ → 0.2392 YMn_2O_5 + 0.05466 $Mn_8Cl_3O_{10}$ + 0.5466 MnO_2 + 0.02957 WO_3 + 1.449 LiCl	−15.00
	LYWC2	0.7382 $LiMn_2O_4$ + 0.2618 $Li_{2.52}Y_{0.84}W_{0.16}Cl_6$ → 0.2199 YMn_2O_5 + 0.05759 $Mn_8Cl_3O_{10}$ + 0.5759 MnO_2 + 0.04188 WO_3 + 1.398 LiCl	−15.00
	LYWC3	0.7462 $LiMn_2O_4$ + 0.2538 $Li_{2.34}Y_{0.78}W_{0.22}Cl_6$ → 0.198 YMn_2O_5 + 0.06091 $Mn_8Cl_3O_{10}$ + 0.6091 MnO_2 + 0.05584 WO_3 + 1.34 LiCl	−15.00
	LYWC4	0.7596 $LiMn_2O_4$ + 0.2404 $Li_{2.01}Y_{0.67}W_{0.33}Cl_6$ → 0.1611 YMn_2O_5 + 0.06651 $Mn_8Cl_3O_{10}$ + 0.6651 MnO_2 + 0.07933 WO_3 + 1.243 LiCl	−15.00
	Li_3PS_4	0.5 Li_3PS4 + 0.5 $LiMn_2O_4$ → 0.5 Li_3PO_4 + 0.5 $Li(MnS_2)_2$	−347.00
	$Li_{10}Ge(PS_6)_2$	0.3333 $Li_{10}Ge(PS_6)_2$ + 0.6667 $LiMn_2O_4$ → 0.3333 Li_4GeS_4 + 0.6667 $Li(MnS_2)_2$ + 0.6667 Li_3PO_4	−280.00
	Li_6PS_5Cl	0.5 Li_6PS_5Cl + 0.5 $LiMn_2O_4$ → 0.5 Li_3PO_4 + 0.5 $Li(MnS_2)_2$ + 0.5 Li_2S + 0.5 LiCl	−316.00

Table S7 Chemical reactions, decomposition phases, and decomposition energy (E_D), between LYWC, sulfides (Li_3PS_4, $Li_{10}Ge(PS_6)_2$, and Li_6PS_5Cl), and cathode materials $Li(NiMnCo)_{1/3}O_2$ (NCM).

Cathode	SSE	Reaction equation	E_D (meV atom^{-1})
NCM	LYC	0.5215 $Li_3MnCoNiO_6$ + 0.4785 Li_3YCl_6 → 0.07975 $Mn(Ni_3O_4)_2$ + 0.04294 $Li_2Mn_3NiO_8$ + 0.1043 $Li_4MnCo_5O_{12}$ + 0.3742 YClO + 0.1043 YMn_2O_5 + 2.497 LiCl	−43.00
	LYWC1	0.5917 $Li_3MnCoNiO_6$ + 0.4083 $Li_{2.67}Y_{0.89}W_{0.11}Cl_6$ → 0.04873 $Li_2Mn_3NiO_8$ + 0.1183 $Li_4MnCo_5O_{12}$ + 0.0905 $Mn(Ni_3O_4)_2$ + 0.04491 Y_2WO_6 + 0.1183 YMn_2O_5 + 0.1552 YClO + 2.294 LiCl	−50.00
	LYWC2	0.6173 $Li_3MnCoNiO_6$ + 0.3827 $Li_{2.52}Y_{0.84}W_{0.16}Cl_6$ → 0.05083 $Li_2Mn_3NiO_8$ + 0.1235 $Li_4MnCo_5O_{12}$ + 0.09441 $Mn(Ni_3O_4)_2$ + 0.06124 Y_2WO_6 + 0.1235 YMn_2O_5 + 0.07556 YClO + 2.221 LiCl	−53.00
	LYWC3	0.6437 $Li_3MnCoNiO_6$ + 0.3563 $Li_{2.34}Y_{0.78}W_{0.22}Cl_6$ → 0.05685 $Li_2Mn_3NiO_8$ + 0.1283 $Li_4MnCo_5O_{12}$ + 0.0978 $Mn(Ni_3O_4)_2$ + 0.002366 Mn_2CoO_4 + 0.0784 Y_2WO_6 + 0.1212 YMn_2O_5 + 2.138 LiCl	−56.00
	LYWC4	0.5345 $Li_3MnCoNiO_6$ + 0.4655 $Li_{2.01}Y_{0.67}W_{0.33}Cl_6$ → 0.07126 $Li_2Mn_3NiO_8$ + 0.1069 $Li_4MnCo_5O_{12}$ + 0.05112 $NiWO_4$ + 0.1025 Y_2WO_6 + 0.1069 YMn_2O_5 + 0.4121 $NiCl_2$ + 1.969 LiCl	−61.00
	Li_3PS_4	0.6 Li_3PS_4 + 0.4 Li3MnCoNiO6 → 0.6 Li_3PO_4 + 0.1333 $Li(MnS_2)_2$ + 0.1333 $Co(NiS_2)_2$ + 0.1333 Co_2NiS_4 + 0.1333 MnS_2 + 0.5333 Li_2S	−407.00
	$Li_{10}Ge(PS_6)_2$	0.317 $Li_{10}Ge(PS_6)_2$ + 0.683 $Li_3MnCoNiO_6$ → 0.317 Li_2MnGeO_4 + 0.2277 $Co(NiS_2)_2$ + 0.6339	−344.00

	Li_6PS_5Cl	$Li_3PO_4 + 0.183\ Li(MnS_2)_2 + 0.07366\ Li_2SO_4 + 0.2277\ Co_2NiS_4 + 1.176\ Li_2S$ $0.4\ Li_3MnCoNiO_6 + 0.6\ Li_6PS_5Cl \rightarrow 0.1333\ Co_2NiS_4 + 0.1333\ Li(MnS_2)_2 + 0.1333\ Co(NiS_2)_2 + 0.1333\ MnS_2 + 1.133\ Li_2S + 0.6\ LiCl + 0.6\ Li_3PO_4$	−364.00

Table S8 Chemical reactions, decomposition phases, and decomposition energy (E_D), between LYWC, sulfides (Li_3PS_4, $Li_{10}Ge(PS_6)_2$, and Li_6PS_5Cl), and cathode materials $LiCoO_2$ (LCO).

Cathode	SSE	Reaction equation	E_D (meV atom^{-1})
LCO	LYC	$0.2857\ Li_3YCl_6 + 0.7143\ LiCoO_2 \rightarrow 0.1429\ Li(CoO_2)_2 + 0.2857\ YClO + 0.1429\ Co_3O_4 + 1.429\ LiCl$	−23.00
	LYWC1	$0.7688\ LiCoO_2 + 0.2312\ Li_{2.67}Y_{0.89}W_{0.11}Cl_6 \rightarrow 0.1538\ Li(CoO_2)_2 + 0.02543\ Y_2WO_6 + 0.1538\ Co_3O_4 + 1.232\ LiCl + 0.1549\ YClO$	−29.00
	LYWC2	$0.7872\ LiCoO_2 + 0.2128\ Li_{2.52}Y_{0.84}W_{0.16}Cl_6 \rightarrow 0.1574\ Li(CoO_2)_2 + 0.03404\ Y_2WO_6 + 0.1574\ Co_3O_4 + 1.166\ LiCl + 0.1106\ YClO$	−31.00
	LYWC3	$0.8058\ LiCoO_2 + 0.1942\ Li_{2.34}Y_{0.78}W_{0.22}Cl_6 \rightarrow 0.1612\ Li(CoO_2)_2 + 0.04272\ Y_2WO_6 + 0.1612\ Co_3O_4 + 1.099\ LiCl + 0.06602\ YClO$	−34.00
	LYWC4	$0.8326\ LiCoO_2 + 0.1674\ Li_{2.01}Y_{0.67}W_{0.33}Cl_6 \rightarrow 0.1665\ Li(CoO_2)_2 + 0.05523\ Y_2WO_6 + 0.1665\ Co_3O_4 + 1.003\ LiCl + 0.001674\ YClO$	−37.00
	Li_3PS_4	$0.3143\ Li_3PS_4 + 0.6857\ LiCoO_2 \rightarrow 0.3143\ Li_3PO_4 + 0.02857\ Li_2SO_4 + 0.2286\ Co_3S_4 + 0.3143\ Li_2S$	−385.00
	$Li_{10}Ge(PS_6)_2$	$0.1037\ Li_{10}Ge(PS_6)_2 + 0.8963\ LiCoO_2 \rightarrow 0.1037\ Li_4GeO_4 + 0.09959\ Co_9S_8 + 0.2075$	−325.00

	$Li_3PO_4 + 0.1369\ Li_2SO_4 + 0.3112\ Li_2S$	
Li_6PS_5Cl	$0.3143\ Li_6PS_5Cl + 0.6857\ LiCoO_2 \rightarrow 0.3143\ Li_3PO_4 + 0.6286\ Li_2S + 0.02857\ Li_2SO_4 + 0.2286\ Co_3S_4 + 0.3143\ LiCl$	−325.00

Table S9 Structure parameters of Li_3YCl_6.

Space group: *P*321

a = b = 11.1867 Å, c = 6.1423 Å.

Atom	Wyckoff position	Atomic coordinates		
		x	y	z
Cl1	6g	0.11460	0.88281	0.77312
Cl7	6g	0.10682	0.56058	0.75463
Cl13	6g	0.21150	0.77178	0.26715
Li1	3f	0.00000	0.67843	0.50000
Li4	3e	0.00000	0.66117	−0.00000
Li7	3e	0.65725	0.65725	−0.00000
Y1	2d	0.33333	0.66667	0.50888
Y3	1a	0.00000	0.00000	0.00000

Table S10 Structure parameters of $Li_{2.67}Y_{0.89}W_{0.11}Cl_6$.

Space group: *P*3

a = b = 11.2469 Å, c = 18.4231 Å.

Atom	Wyckoff position	Atomic coordinates		
		x	y	z
Cl1	3d	0.12497	0.88942	0.26076
Cl4	3d	0.88540	0.11840	0.74203
Cl7	3d	0.10988	0.87798	0.59297
Cl10	3d	0.00000	0.67843	0.50000
Cl13	3d	0.00000	0.66117	−0.00000
Cl16	3d	0.65725	0.65725	−0.00000
Cl19	3d	0.33333	0.66667	0.50888
Cl22	3d	0.00000	0.00000	0.00000

Cl25	3d	0.21120	0.76859	0.76859
Cl28	3d	0.76347	0.23624	0.22880
Cl31	3d	0.21205	0.76911	0.76058
Cl34	3d	0.76764	0.21069	0.57200
Cl37	3d	0.11022	0.55350	0.25381
Cl40	3d	0.56216	0.10645	0.74931
Cl43	3d	0.10619	0.55508	0.59038
Cl46	3d	0.57085	0.13981	0.08530
Cl49	3d	0.10363	0.56436	0.92251
Cl52	3d	0.56231	0.10850	0.40678
Li1	3d	0.99063	0.68949	0.49625
Li4	3d	0.99571	0.67323	0.83619
Li7	3d	0.04138	0.70015	0.01119
Li10	3d	0.03548	0.67654	0.32908
Li13	3d	0.98162	0.65101	0.66298
Li16	3d	0.67165	0.67278	0.98778
Li19	3d	0.64012	0.67130	0.34494
Li22	3d	0.64460	0.66787	0.67922
Y1	1b	0.33333	0.66667	0.16783
Y2	1b	0.33333	0.66667	0.51343
Y3	1b	0.33333	0.66667	0.84283
Y4	1c	0.66667	0.33333	0.83072
Y5	1c	0.66667	0.33333	0.48980
Y6	1a	0.00000	0.00000	0.00344
Y7	1a	0.00000	0.00000	0.32881
Y8	1a	0.00000	0.00000	0.66764
W1	1c	0.66667	0.33333	0.15898

Table S11 Structure parameters of $Li_{2.52}Y_{0.84}W_{0.16}Cl_6$.

Space group: *P*3

a = b = 11.2688 Å, c = 12.2188 Å.

Atom	Wyckoff position	Atomic coordinates		
		x	y	z
Cl1	3d	0.12701	0.89307	0.39400

Cl4	3d	0.87489	0.11059	0.61114
Cl7	3d	0.11150	0.88552	0.88077
Cl10	3d	0.87844	0.11500	0.10517
Cl13	3d	0.24303	0.79757	0.12839
Cl16	3d	0.77482	0.22000	0.86256
Cl19	3d	0.21491	0.77054	0.64437
Cl22	3d	0.76327	0.23639	0.34498
Cl25	3d	0.10990	0.55531	0.38312
Cl28	3d	0.56294	0.10733	0.61447
Cl31	3d	0.10161	0.56325	0.88554
Cl34	3d	0.57111	0.14024	0.12861
Li1	3d	0.98939	0.67876	0.75125
Li4	3d	0.04436	0.70203	0.01844
Li7	3d	0.03647	0.68024	0.49637
Li10	3d	0.67423	0.67063	0.97963
Li13	3d	0.63976	0.66977	0.51843
Y1	1b	0.33333	0.66667	0.25399
Y2	1b	0.33333	0.66667	0.77172
Y3	1c	0.66667	0.33333	0.73743
Y4	1a	0.00000	0.00000	0.00618
Y5	1a	0.00000	0.00000	0.49932
W1	1c	0.66667	0.33333	0.23960

Table S12 Structure parameters of $Li_{2.34}Y_{0.78}W_{0.22}Cl_6$.

Space group: *P*321

a = b = 11.2941 Å, c = 18.1226 Å.

Atom	Wyckoff position	Atomic coordinates		
		x	y	z
Cl1	6g	0.11280	0.88713	0.42065
Cl7	6g	0.87918	0.11178	0.90553
Cl13	6g	0.12436	0.88837	0.75908
Cl19	6g	0.23680	0.76310	0.26495
Cl25	6g	0.76740	0.21193	0.07209
Cl31	6g	0.22293	0.77586	0.57375

Cl37	6g	0.14017	0.57017	0.41067
Cl43	6g	0.55861	0.10702	0.90554
Cl49	6g	0.11209	0.55276	0.74906
Li1	6g	0.96414	0.63861	0.17380
Li7	6g	0.67330	0.63980	0.15845
Li13	3e	−0.00000	0.70715	0.00000
Li16	3f	−0.00000	0.69329	0.50000
Li19	3f	0.69343	0.69343	0.50000
Y1	2d	0.33333	0.66667	0.66092
Y3	2d	0.66667	0.33333	0.98449
Y5	2c	0.00000	0.00000	0.17251
Y7	1b	0.00000	0.00000	0.50000
W1	2d	0.33333	0.66667	0.33715

Table S13 Structure parameters of $Li_{2.01}Y_{0.67}W_{0.33}Cl_6$.

Space group: *P*3

a = b = 11.0873 Å, c = 6.1125 Å.

Atom	Wyckoff position	Atomic coordinates		
		x	y	z
Cl1	3d	0.15236	0.93556	0.71424
Cl4	3d	0.83577	0.06753	0.17575
Cl7	3d	0.26721	0.81743	0.23607
Cl110	3d	0.76527	0.23711	0.62991
Cl13	3d	0.10126	0.59606	0.70054
Cl16	3d	0.56494	0.13849	0.19198
Li1	3d	0.06864	0.75591	0.45989
Li4	3d	0.10781	0.75337	0.95785
Y1	1b	0.33333	0.66667	0.48424
Y2	1a	1.00000	1.00000	0.96260
W1	1c	0.66667	0.33333	0.40971

Exclusion of the 600 K data point

For the LYWC4 structure, the Li^+ mean square displacement (MSD) at 600 K did not show long-range diffusion (MSD < 10 Å within 200 ps) (Fig. S15 (e)†), we excluded this data point from the linear fit.

References

1. Y. Wang, Z. Ren, J. Zhang, S. Lu, C. Hua, H. Yuan, J. Luo, Y. Liu, J. Nai and X. Tao, *Adv. Sci.*, 2024, **11**, 2404213.

2. F. Li, X. Cheng, L. L. Lu, Y. C. Yin, J. D. Luo, G. Lu, Y. F. Meng, H. Mo, T. Tian, J. T. Yang, W. Wen, Z. P. Liu, G. Zhang, C. Shang and H. B. Yao, *Nano Lett.*, 2022, **22**, 2461-2469.

3. X. Li, J. Liang, X. Yang, K. R. Adair, C. Wang, F. Zhao and X. Sun, *Energy Environ. Sci.*, 2020, **13**, 1429-1461.

4. S. Wang, Q. Bai, A. M. Nolan, Y. Liu, S. Gong, Q. Sun and Y. Mo, *Angew. Chem. Int. Ed.*, 2019, **58**, 8039-8043.

5. X. Fu, Y. Wang, J. Xu, Q. Yang, H. Mao, R. Xiao and H. Li, *J. Mater. Chem. A*, 2024, **12**, 10562-10570.

6. Y. Ren, C. Sun, J. Liu, G. Cai, X. Tan and C. Zhang, *Mater. Today Commun.*, 2022, **33**, 104570.

7. X. Shi, Z. Zeng, H. Zhang, Y. Huang, C. H. Yan and Y. Du, *Adv. Funct. Mater.*, 2023, **33**, 2213638.

8. B. Singh, Y. Wang, J. Liu, J. D. Bazak, A. Shyamsunder and L. F. Nazar, *J. Am. Chem. Soc.*, 2024, **146**, 17158-17169.

9. A. Jain, S. P. Ong, G. Hautier, W. Chen, W. D. Richards, S. Dacek, S. Cholia, D. Gunter, D. Skinner, G. Ceder and K. A. Persson, *APL Mater.*, 2013, **1**, 011002.

10. M. Jiang, Z. W. Chen, A. Rao, L. X. Chen, X. T. Zu and C. V. Singh, *J. Mater. Chem. C*, 2022, **10**, 18294-18302.

11. N. Kamaya, K. Homma, Y. Yamakawa, M. Hirayama, R. Kanno, M. Yonemura, T. Kamiyama, Y. Kato, S. Hama, K. Kawamoto and A. Mitsui, *Nat. Mater.*, 2011, **10**, 682-686.